Self-Activated Electrical Stimulation for Effective Hair Regeneration *Via* a Wearable Omnidirectional Pulse Generator

Guang Yao,[†,§,#] *Dawei Jiang,*[‡,⁄⁄,#] *Jun Li,*[†] *Lei Kang,*[‡] *Sihong Chen,*[§] *Yin Long,*[†,§] *Yizhan Wang,*[†] *Peng Huang,*[⁄⁄] *Yuan Lin,*[§] *Weibo Cai,*[*,‡] *Xudong Wang*[*,†]

[†]Department of Materials Science and Engineering, University of Wisconsin-Madison, Madison, Wisconsin 53706, USA.

[‡]Department of Radiology, University of Wisconsin-Madison, Madison, Wisconsin 53705, USA.

[§]State Key Laboratory of Electronic Thin films and Integrated Devices, University of Electronic Science and Technology of China, Chengdu, Sichuan 610054, P. R. China.

[⁄⁄]Guangdong Key Laboratory for Biomedical Measurements and Ultrasound Imaging, Carson International Cancer Center, Laboratory of Evolutionary Theranostics, School of Biomedical Engineering, Health Science Center, Shenzhen University, Shenzhen 518060, China

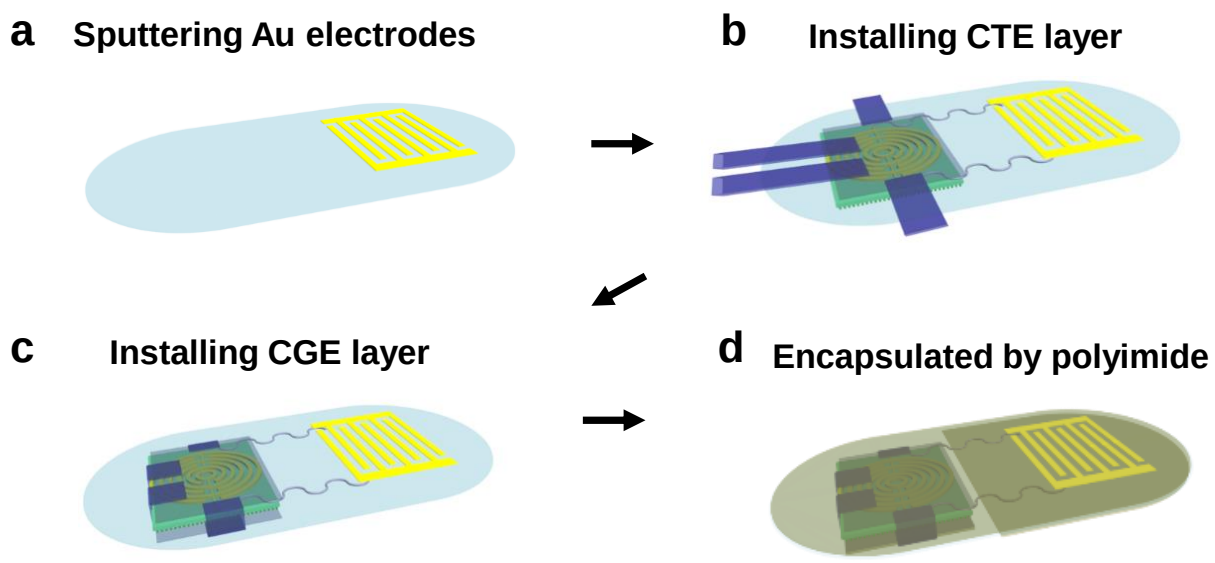

Figure S1. The detailed fabrication process of the *m*-ESD. (a) PET substrate was prepared and sputtered with Au film to fabricate the interdigitated electrodes. **(b)** The CTE was installed on the PET substrate as the CTE layer. **(c)** The CGE was assembled together with the CTE layer to fabricate the *m*-ESD. **(d)** The *m*-ESD was encapsulated with a biocompatible polyimide film.

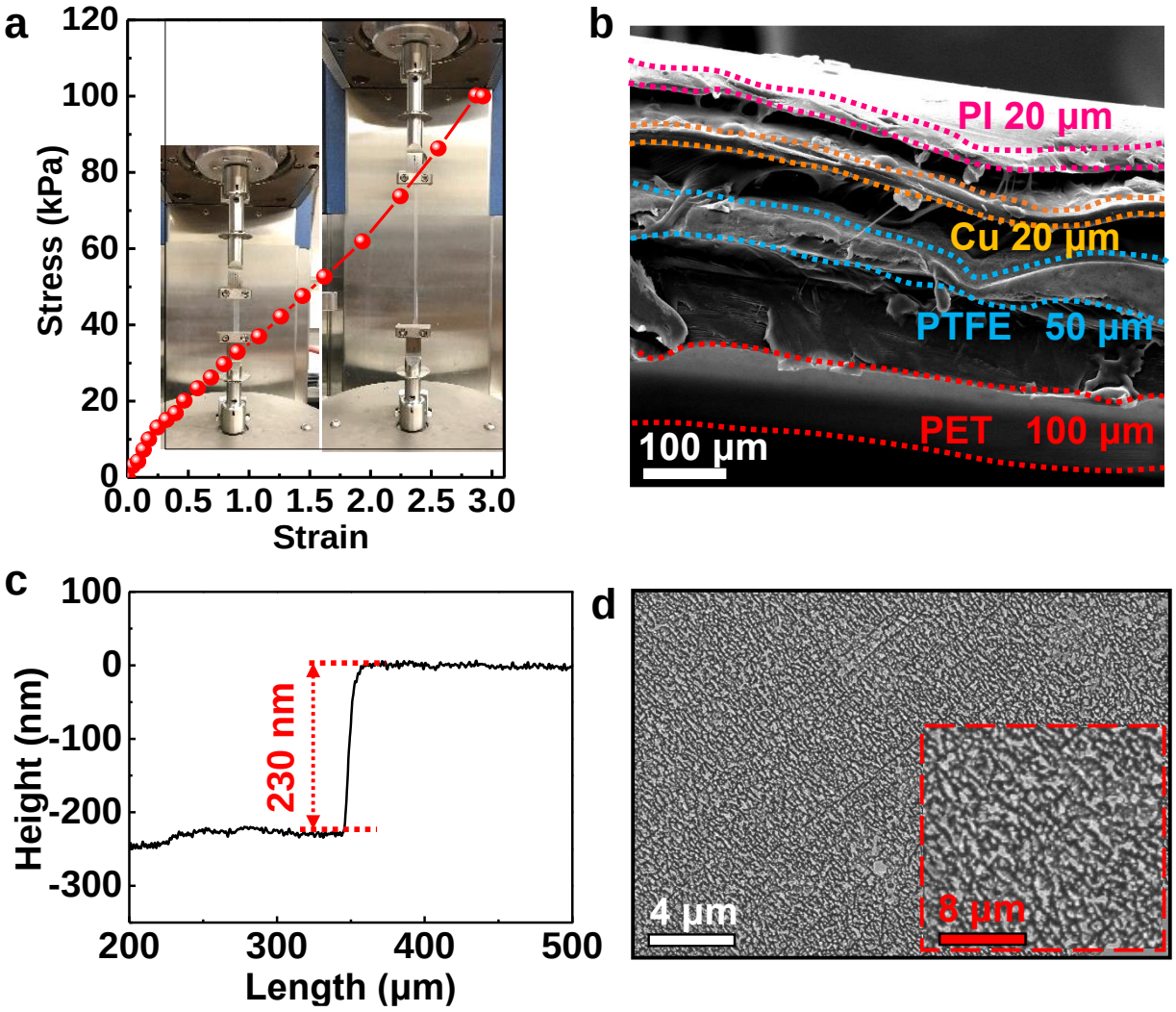

Figure S2. Performance characterization of the Ecoflex band and *m*-ESD. (a) Stress-strain curve of the soft Ecoflex band. **(b)** Cross-section SEM photos of the m-ESD. **(c)** The thickness of Au electrode tested by a step profiler. **(d)** SEM photo of nanostructured PTFE film.

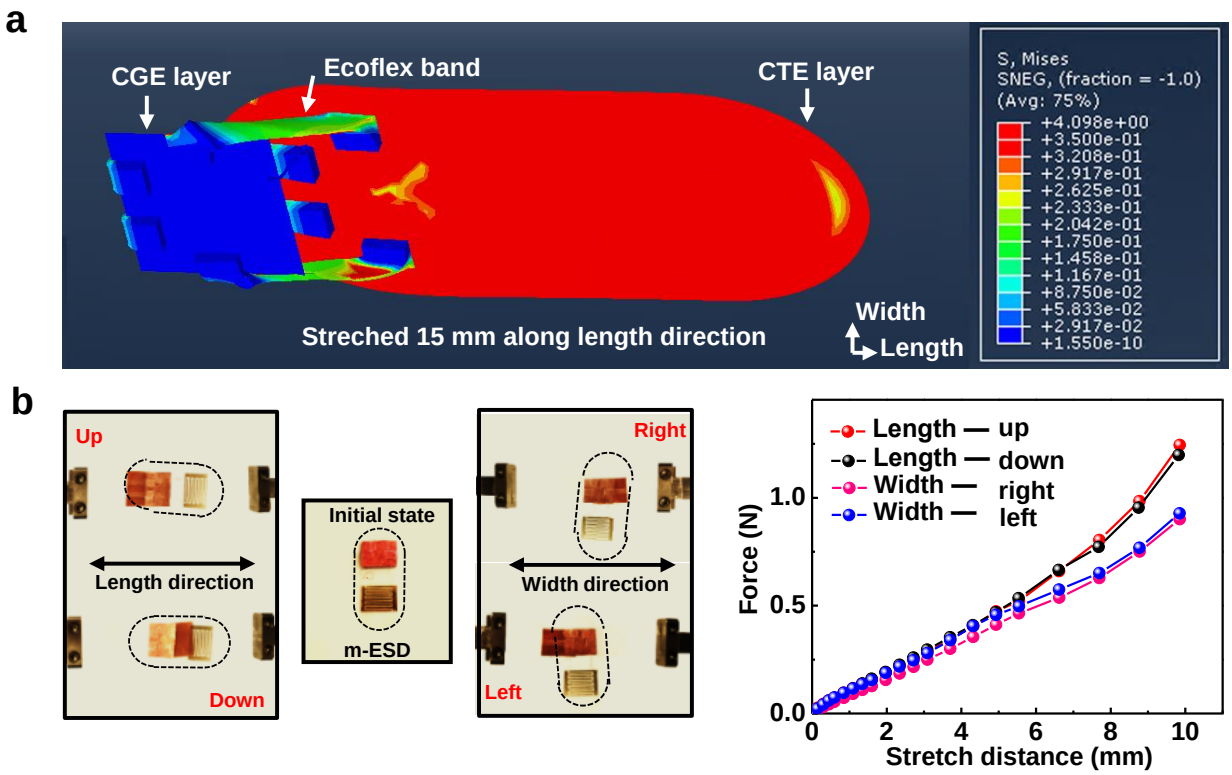

Figure S3. Computational and experimental mechanical properties of the *m*-ESD. (a) Finite element analysis when the *m*-ESD was stretched 15 mm along the length direction (The CGE layer was fixed). During the stretching process, the strain was primarily distributed on the Ecoflex bands while the stress is mainly concentrated on the CTE layer. **(b)** Optical photos and force-distance curves when the *m*-ESD was stretched along the length and width directions.

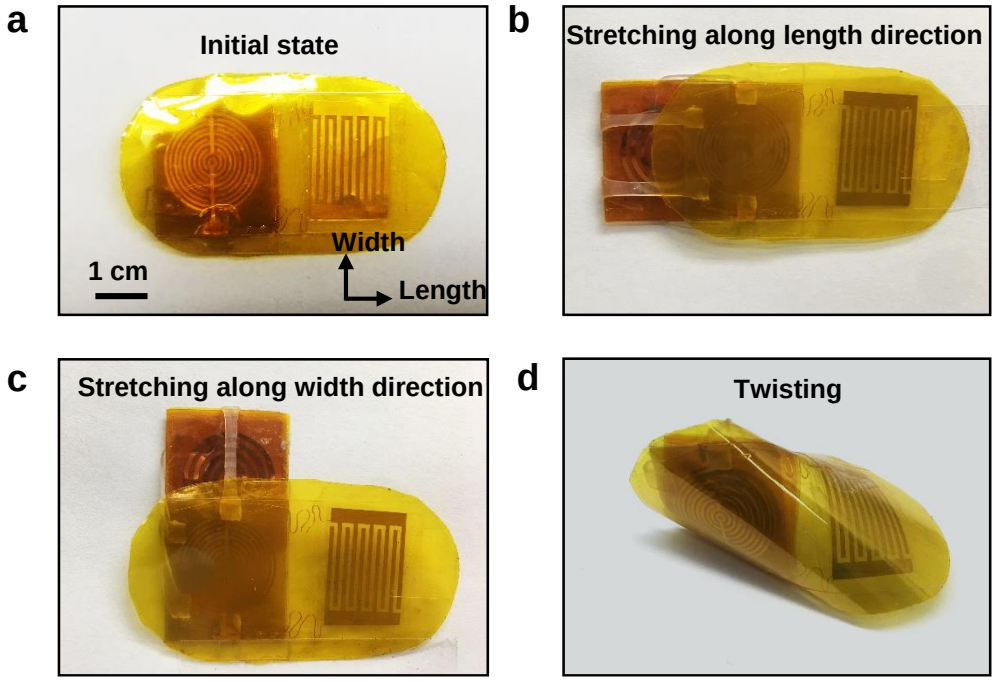

Figure S4. Mechanical compliance and robustness of the *m*-ESD. Optical photos of the *m*-ESD under initial state **(a)**, stretching along length direction **(b)**, stretching along width direction **(c)** and twisting **(d)**.

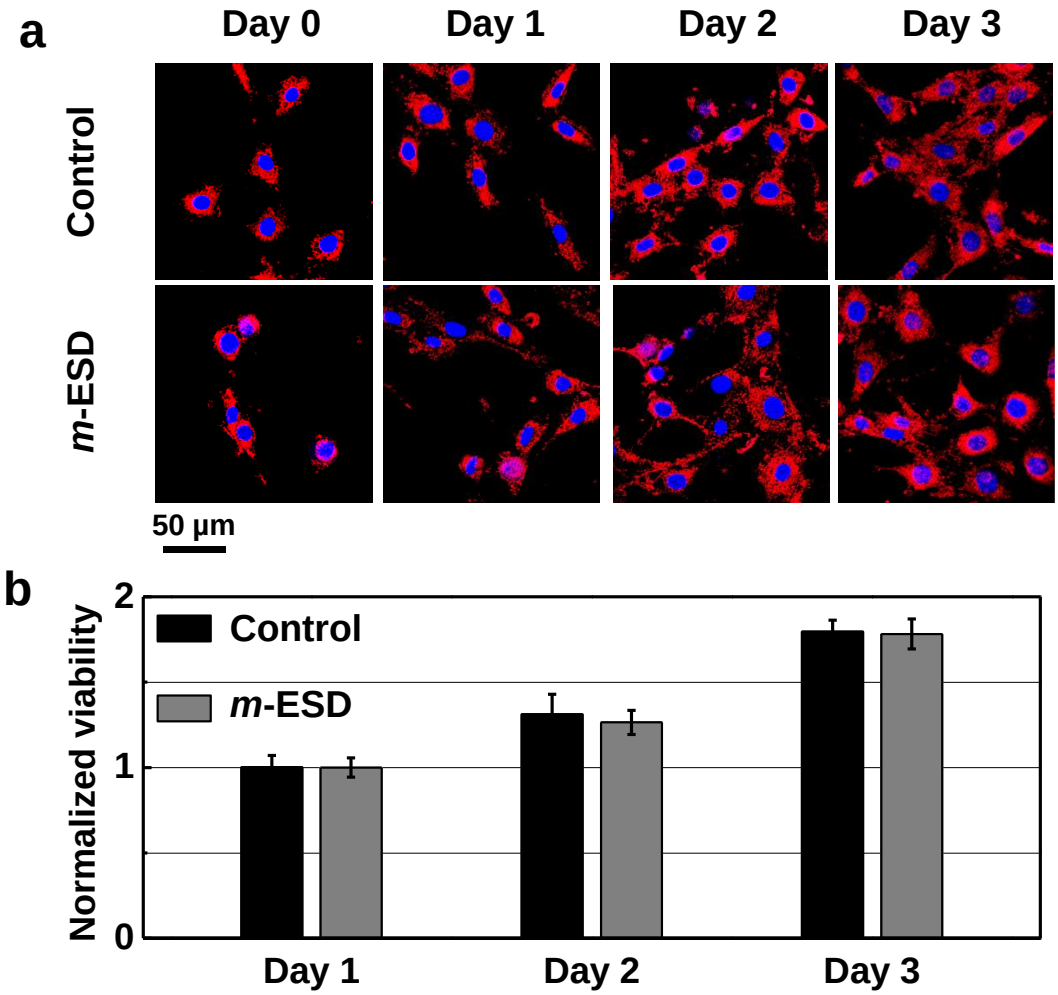

Figure S5. Biocompatible performance of the *m*-ESD. (a) Fluorescence images of stained 3T3 cells that were cultured on a cell culture dish and on the surface of the *m*-ESD. **(b)** Comparison of normalized cell viability for 3 days showing the *m*-ESD is non-cytotoxic and biocompatible.

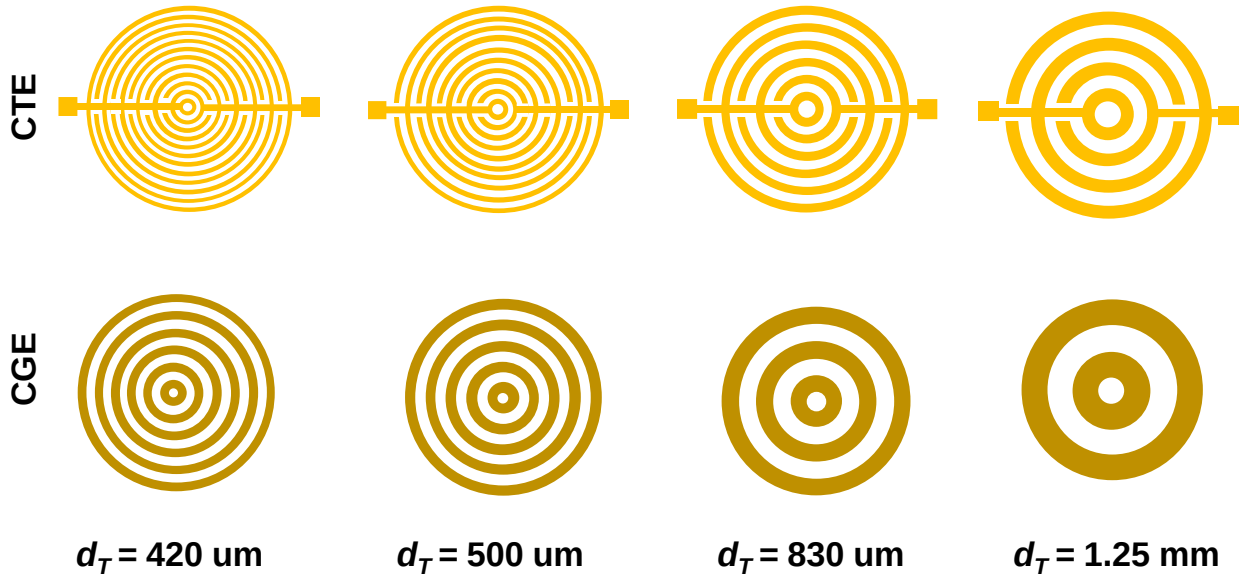

Figure S6. Four different configurations of CTE and corresponding CGE.

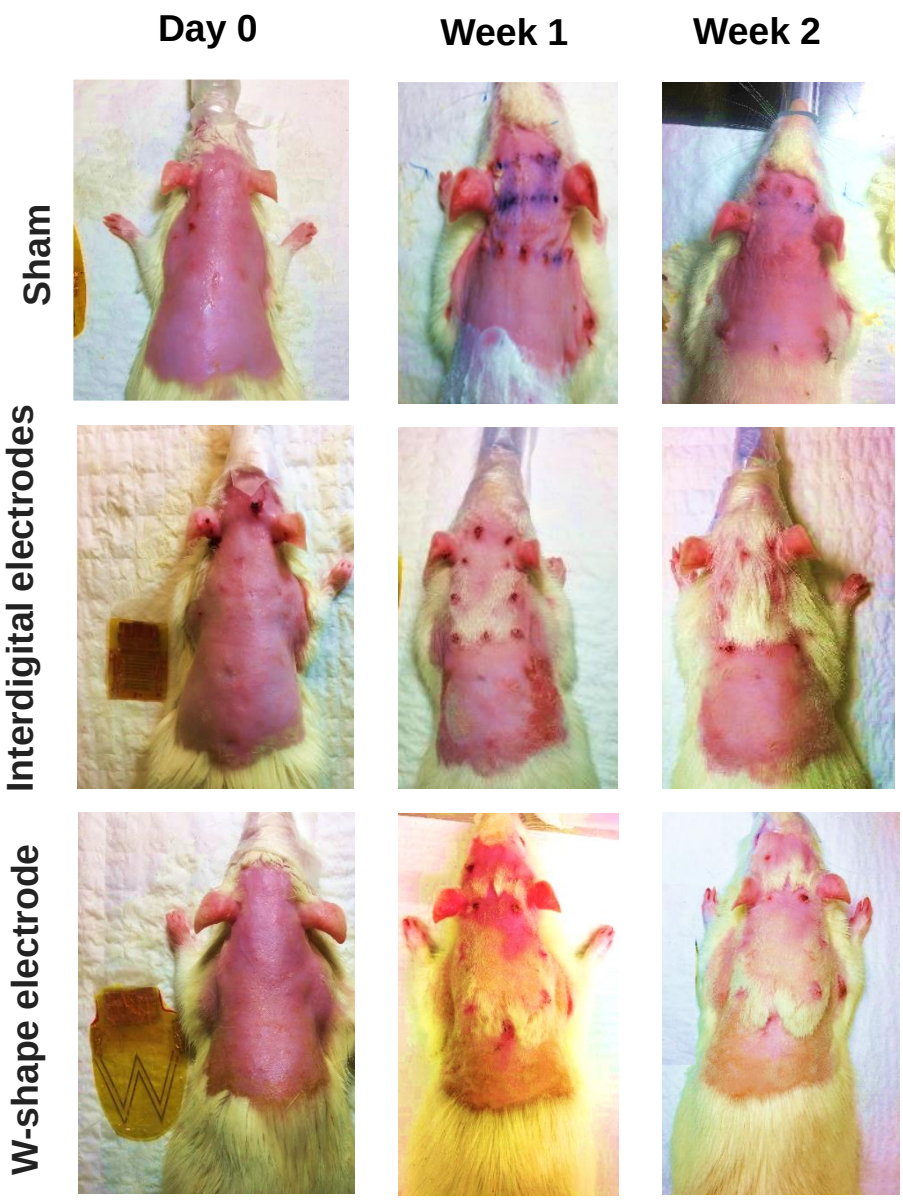

Figure S7. Images of the rat treated with sham *m*-ESD and *m*-ESD with interdigitated and W-shaped electrodes, respectively.

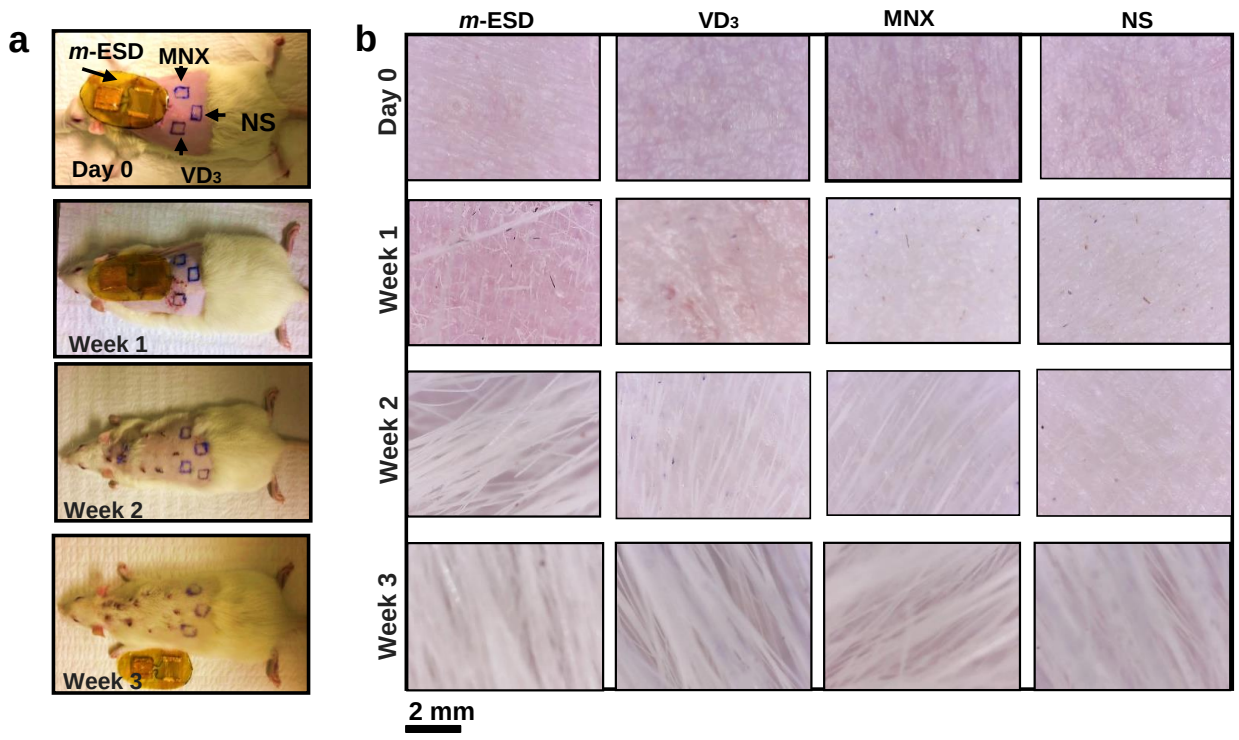

Figure S8. Hair regeneration under different stimulation methods. (a) Comparison of hair regeneration under the influence of *m*-ESD, MNX, VD_3 and NS. **(b)** Images of hair in different regions with a handheld digital microscope.

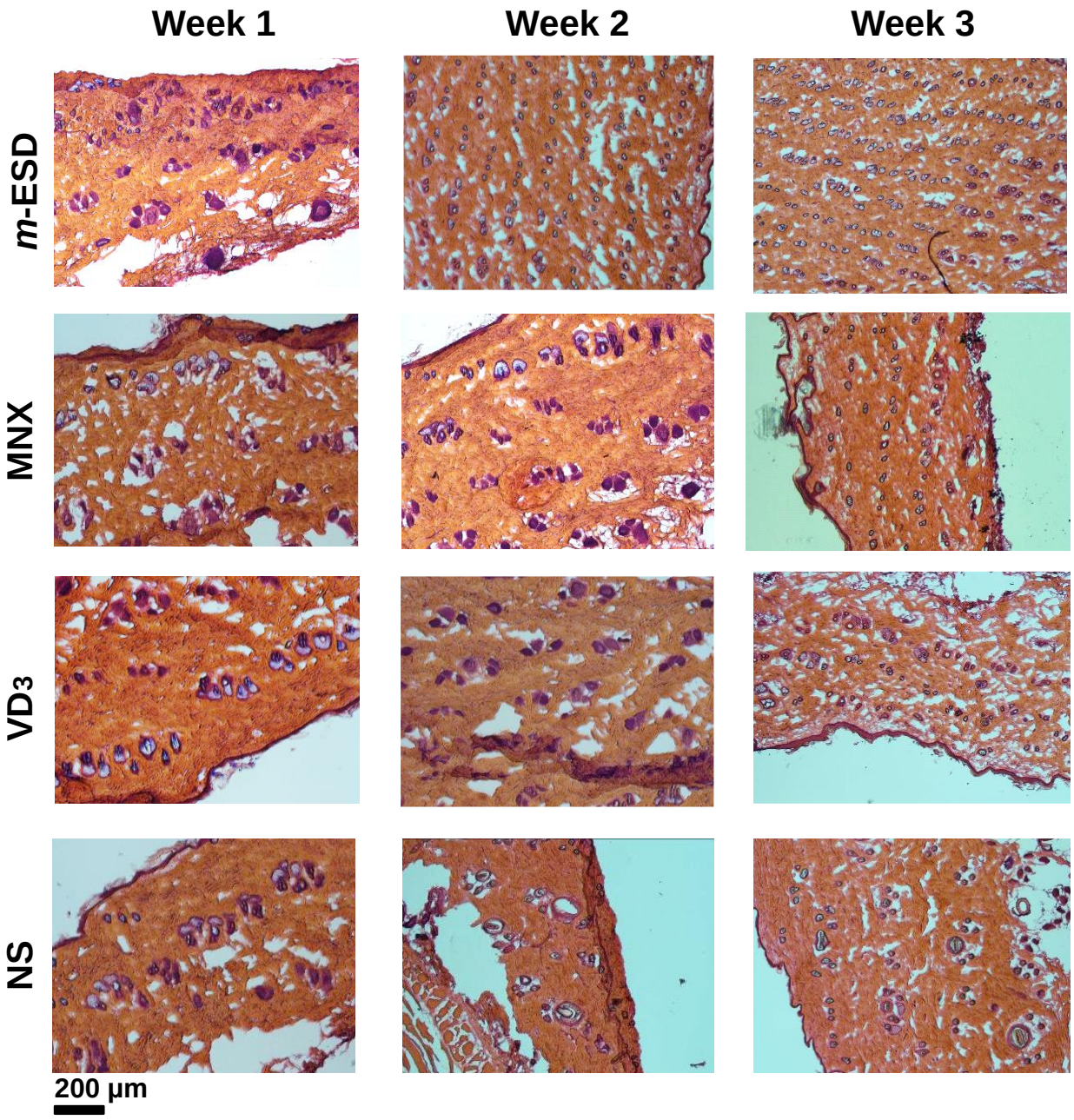

Figure S9. H&E staining of horizontal slices in different regions for SD rats.

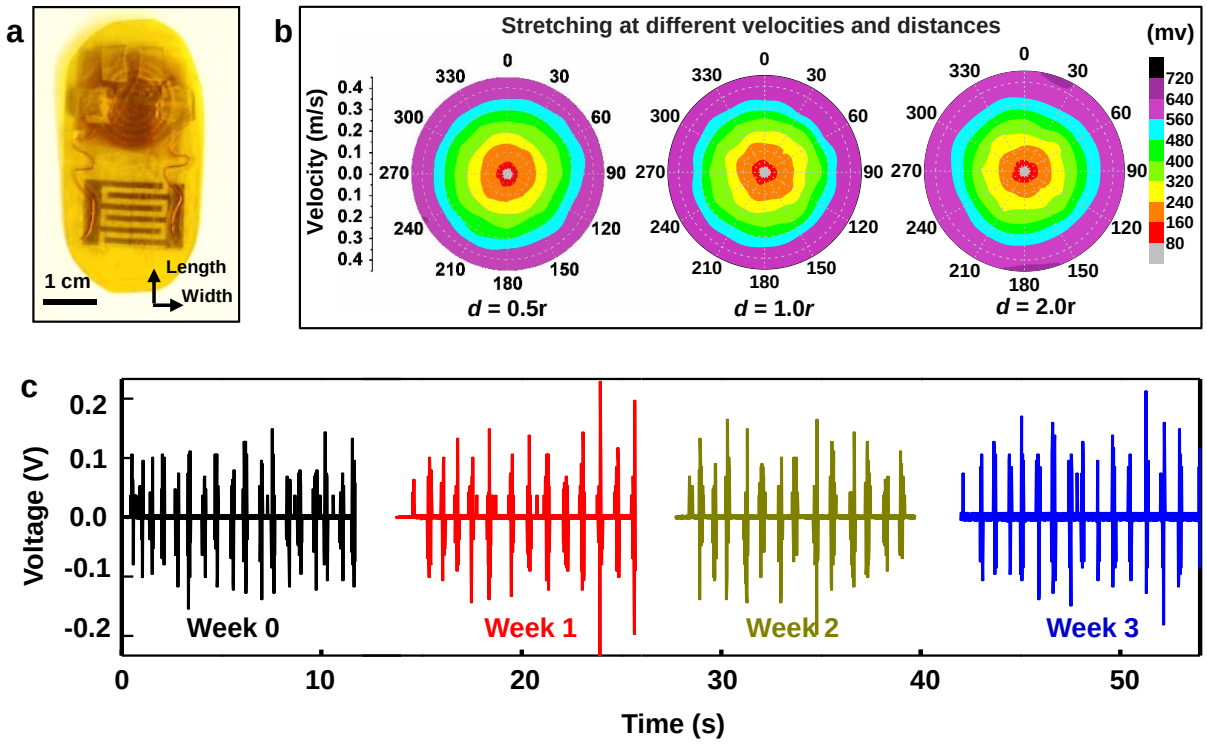

Figure S10. The *m*-ESD for nude mice. (a) Optical image of the *m*-ESD. **(b)** Voltage output of the *m*-ESD stretching at different directions, velocities and distances (*d* is the displacement distance and *r* represents the electrode radius). **(c)** Long-period stability test of the m-ESD on mice.

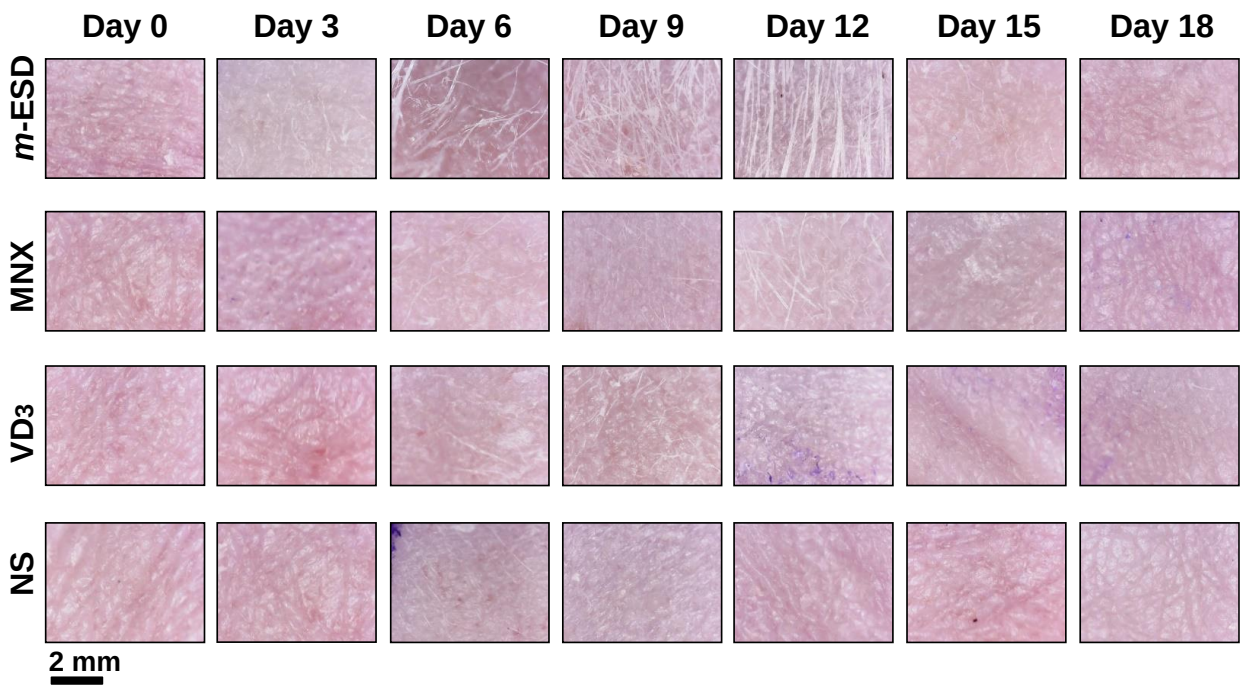

Figure S11. Images of hair under the influence of *m*-ESD, MNX, VD3 and NS with a handheld digital microscope.

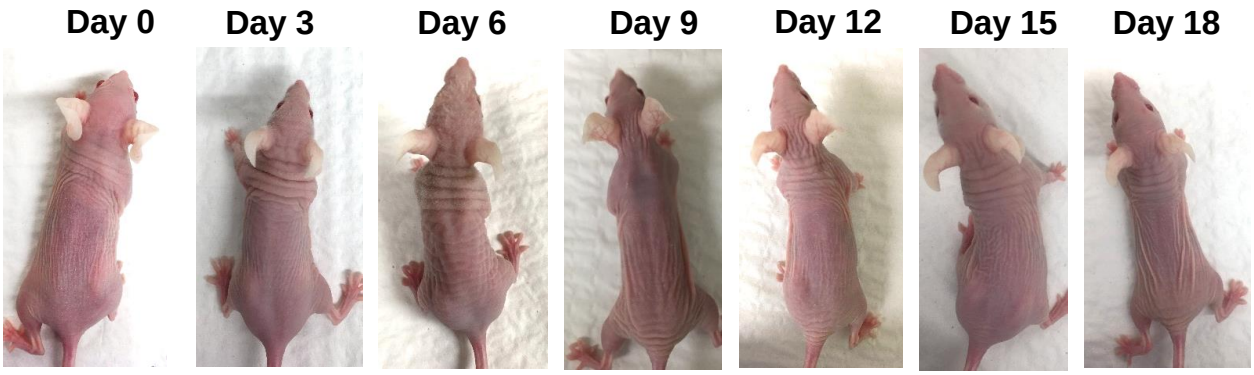

Figure S12. Optical images of nude mice without treatment.

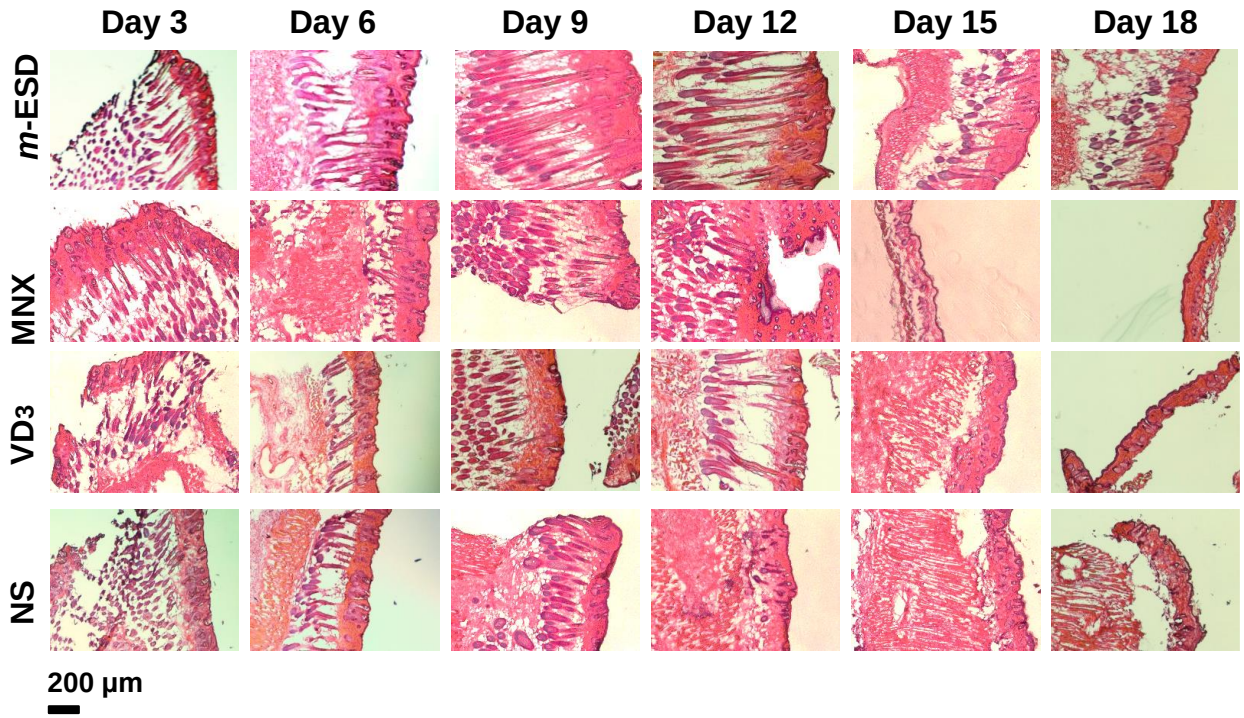

Figure S13. H&E staining of longitudinal slices of the epidermis under different stimulation time for nude mice.

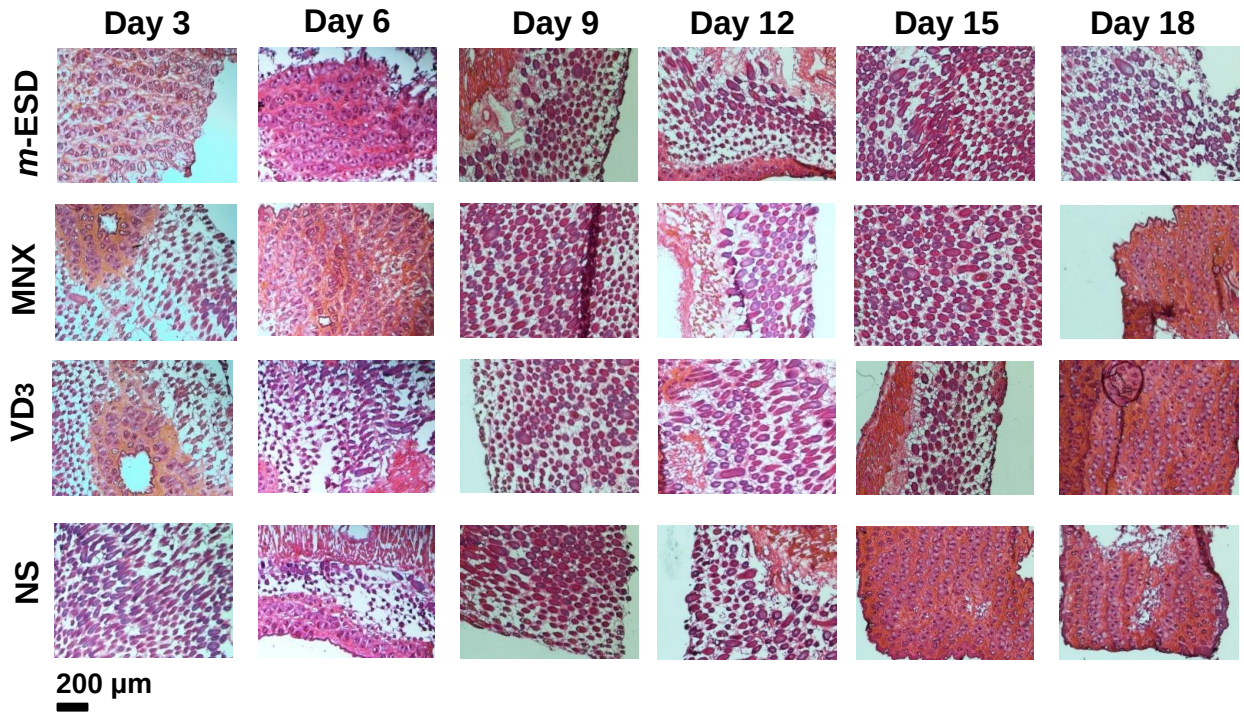

Figure S14. H&E staining of horizontal slices over time for nude mice.